Chapter 17

Analysis of Plant Mitochondrial Function Using Fluorescent Protein Sensors

Stephan Wagner, Thomas Nietzel, Isabel Aller, Alex Costa, Mark D. Fricker, Andreas J. Meyer, and Markus Schwarzländer

Abstract

Mitochondrial physiology sets the basis for function of the organelle and vice versa. While a limited range of in vivo parameters, such as oxygen consumption, has been classically accessible for measurement, a growing collection of fluorescent protein sensors can now give insights into the physiology of plant mitochondria. Nevertheless, the meaningful application of these sensors in mitochondria is technically challenging and requires rigorous experimental standards. Here we exemplify the application of three genetically encoded sensors to monitor glutathione redox potential, pH, and calcium in the matrix of mitochondria in intact plants. We describe current methods for quantitative imaging and analysis in living root tips by confocal microscopy and discuss methodological limitations.

Key words Plant mitochondria, Fluorescent protein sensors, In vivo imaging, Confocal microscopy, Respiratory physiology, roGFP, Cameleon, cpYFP

1 Introduction

While much of the mitochondrial respiratory machinery is known in molecular detail [1], knowledge of the physiological context that it operates in in vivo is still very limited. This is an important issue to overcome if we are to understand how individual or populations of mitochondria function *in planta*. Hallmarks of mitochondrial physiology, such as pH or membrane potential, are not only set by the mitochondrial machinery, but they also control the function of those systems, either through direct regulation or indirectly as signals [2].

Mitochondria maintain a physiological status that differs markedly from the surrounding cytosol and other compartments (e.g. for thiol redox status [3], pH [4], calcium [5], or ATP levels [6]). Both mitochondrial membranes that separate the organelle from the cytosol allow distinct physiological identities of the respective spaces to be maintained. The inner mitochondrial membrane

James Whelan and Monika W. Murcha (eds.), *Plant Mitochondria: Methods and Protocols*, Methods in Molecular Biology, vol. 1305, DOI 10.1007/978-1-4939-2639-8_17,

provides a particularly selective barrier with a pronounced proton motive force allowing the matrix to establish its distinct physiological status. Considering the specific physiology of mitochondria and their sub-compartments separately from other parts of the cell is therefore critical and necessitates a mitochondria-specific readout in the context of the living plant cell.

Fluorescent protein sensors are well suited for measuring mitochondrial physiology and inferring function. As proteins they can be genetically targeted to specific subcellular locations with high accuracy, and their fluorescence allows nondestructive measurements from living cells and tissues of physiological parameters along with and mitochondrial morphology, motility, and localization. Here we provide a guideline for the application of fluorescent protein sensors to explore the specific physiological status in the matrix of plant mitochondria using confocal microscopy. We focus on one sensor for each, glutathione redox potential (E_{GSH}), pH, and free calcium, that have proven adequate for measurements in the mitochondrial matrix [5, 7, 8]. However, the principles of the approach described can be generalized to other fluorescent protein sensors, other physiological parameters, other submitochondrial compartments, or other tissues.

2 Materials

2.1 Sensors, Constructs, and Plant Lines

For all three sensors comprehensive in vitro characterization is available, including a reliable account of their respective spectroscopic characteristics, specificities, and sensitivity ranges (Table 1; *see* **Notes 1–6**). This is a critical prerequisite for their use *in planta*, although it cannot be ruled out that their behavior may alter in the complex in vivo environment. Constructs for Agrobacterium-based plant transformation and stable transgenic lines in Arabidopsis Col-0 (*Arabidopsis thaliana* ecotype Columbia-0) background with confirmed mitochondrial sensor localization (*see* **Notes 7** and **8**) are available upon request [5, 7, 8].

2.2 Plant Culture

Young seedlings (2–5 days after germination) are convenient for mitochondrial imaging due to a high mitochondrial density (and maximal sensor signal in turn), thin tissue layers, and cell walls that are still relatively permeable to external treatments. Whole young seedlings can be used, which avoids cutting tissue, and subsequent potential effects on plant or tissue physiology. Seedlings are cultured on vertical medium plates [0.5× MS medium, pH 5.8 (with KOH), 0.8 % (w/v) phytagel] with the root growing along the medium surface. This allows transfer of the whole seedling with minimal mechanical stress (*see* **Note 8**).

Table 1
Characteristics of three sensors for mitochondrial glutathione redox status (E_{GSH}), pH, and free calcium concentration, and Arabidopsis lines expressing the sensors

Parameter	E_{GSH}	pH	Ca^{2+}
Sensor and line name	mt-roGFP2-Grx1	mt-cpYFP	4mt-YC3.6
Targeting peptide (*see* **Note 7**)	1× SHMT (Arabidopsis)	1× β-ATPase (Nicotiana)	4× COX8 (human)
Promoter (*see* **Note 5**)	UBQ10 (Arabidopsis)	35S (CaMV)	35S (CaMV)
Antibiotic selection in plants (*see* **Note 8**)	Kanamycin	Hygromycin	Hygromycin
50 % response (purified protein)	−280 mV (E_{GSH})	8.7 (pH; at 488 nm excitation)	250 nM [Ca^{2+}]
Physiological range of reliable sensitivity (*see* **Note 1**)	−240 to −320 mV (at pH 7.0)	7–10	50 nM to 1 μM
pH sensitivity (pH 6.5–8.2)	Negligible	Very strong	Minor
Ratioing principle (*see* **Note 3**)	Dual excitation, single emission	Dual excitation, single emission	Single excitation, dual emission (FRET)
FP basis	EGFP	cpYFP	CFP, cpVenus
Excitation maximum	400 nm, 490 nm	418 nm, 494 nm	436 nm
Excitation laser line for microscopy	405 nm, 488 nm	405 nm, 488 nm	442 nm or 458 nm
Emission maximum	511 nm	515 nm	476 nm, 527 nm
Emission range for microscopy	505–530 nm	505–530 nm	475–500 nm, 525–540 nm
Spectroscopic dynamic range (purified protein)	~12	~50 (pH 7–10)	~7
Spectroscopic dynamic range (in Arabidopsis root tip mitochondria)	~5 (Fig. 3)	~20 (pH 7–10; Fig. 3)	>4 (*see* **Note 11**)
References	[7, 13, 15, 22]	[8, 16, 23, 24, 27]	[5, 25, 26]

2.3 Assay Media

Culture medium: 0.5× MS, 10 mM MES, pH 5.8.

Calcium measurement medium: 5 mM KCl, 10 mM $CaCl_2$, 10 mM MES, pH 5.8 [5].

2.4 Imaging Chamber

Live imaging of plant physiology benefits from minimal perturbation to the tissue during measurement. While it is impossible to achieve that entirely, practical compromises can be reached to avoid mechanical stress. A simple imaging chamber is used allowing sufficient space for the tissue between microscope slide and coverslip using 1–3 layers of insulating tape as spacers to match the tissue thickness and to build a hydrophobic barrier for the medium

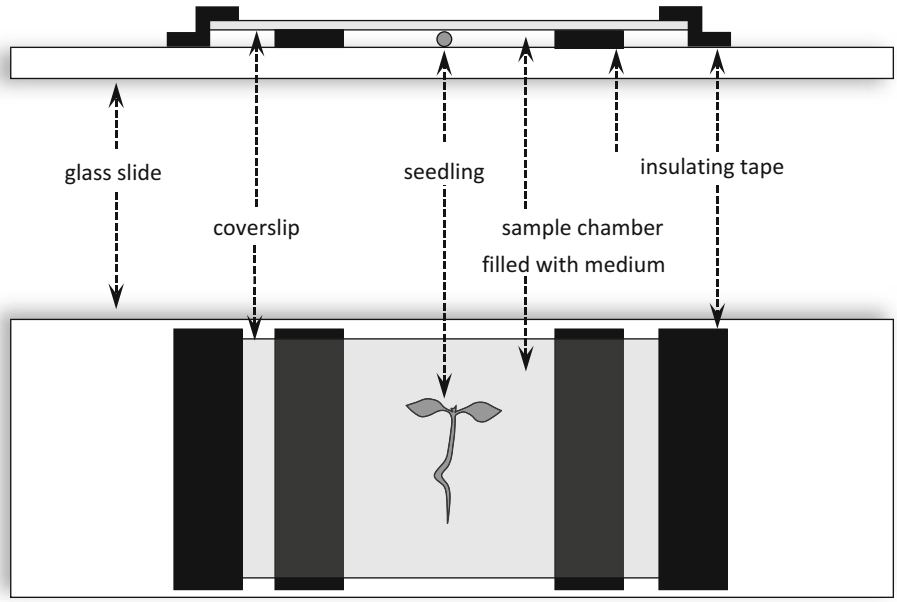

Fig. 1 Schematic side and top view of simple chamber for live imaging

(Fig. 1). Systems for medium exchange or continuous perfusion can be highly useful for dynamic stimulus application and kinetic analysis [9] (*see* **Note 4**) but will not be covered here.

2.5 Confocal Microscope and Laser Settings

A state-of-the-art (upright or inverted) confocal microscope is required for the measurements described here. The method is described for a Zeiss LSM780 confocal system (Carl Zeiss Microscopy GmbH, Jena, Germany), but can be applied at other setups. Laser lines for 405 and 488 nm excitation are required for roGFP2-Grx1 and cpYFP imaging, while a single 442 or 458 nm line is needed for YC3.6 imaging.

2.6 Image Analysis

Careful ratiometric image analysis is critical to extract quantitative data. We have developed a custom MatLab (The MathWorks, Natick, MA) analysis suite that integrates the different analysis and visualization steps via a clear user interface. The program and a detailed user manual are available upon request from Mark D. Fricker, University of Oxford, UK (mark.fricker@plants.ox.ac.uk).

3 Methods

A straightforward procedure is presented here to compare E_{GSH}, pH, and free calcium levels in the mitochondrial matrix at steady state in root tips of young Arabidopsis seedlings between two conditions (e.g. treatment *vs.* control). The aim is to illustrate the principal steps and considerations for routine measurement, which

can then be transferred to other systems and different or more complex tasks, such as monitoring of dynamic changes in the physiology in individual mitochondria [10] or across the mitochondrial populations of whole tissues [5, 11].

3.1 Sample Mounting

1. Gently lift a seedling off the plate using a pair of featherweight forceps and place it in a drop of culture medium (~50 μL) on the microscope slide between the two strips of insulating tape (Fig. 1).
2. Gently place a coverslip on top, avoid air bubbles, and fix it with tape on both sides.
3. If the resulting chamber is not completely filled with medium, carefully top up by pipetting additional medium to one of the open sides.
4. Mount the slide onto the microscope stage. For calcium and pH measurements let the sample rest for 15 min to allow potential touch-induced transients to settle.
5. Choose a lens and add the appropriate immersion liquid. A 25× lens (water immersion, NA 0.8) allows coverage of the entire root tip up to the elongation zone; a 40× lens (water immersion, NA 1.2) allows individual mitochondria to be resolved. Water immersion is best suited optically for plant in vivo imaging, while oil immersion lenses with large numerical aperture can provide good results for tissue layers just below the coverslip at high resolution.
6. Identify the root tip in bright-field mode, and then check for sensor expression using fluorescent light in combination with a green fluorescent protein (GFP) or yellow fluorescent protein (YFP) filter (*see* **Notes 5** and **6**).
7. Use the first specimen to set up the confocal microscope and to optimize the instrument settings. Then start the data collection with a separate set of individuals.

3.2 General Confocal Settings

1. For the roGFP2-Grx1 and cpYFP sensors set up two channels with excitation at 405 and 488 nm, with a dichroic mirror for both excitation wavelengths. Line switching, rather than frame switching, between channels should be used, as mitochondria can be very motile in plants. Sensor fluorescence is detected at 505–530 nm. For the 405 nm channel the emission signal at 430–470 nm is also collected which may be used to correct for autofluorescence. Autofluorescence of cell wall or vacuolar contents can be significant in this channel. For the YC3.6 sensor one channel is set up with excitation at 458 nm (or 442 nm if available for more efficient excitation closer to the CFP excitation maximum (Table 1) [12]) and fluorescence is collected at 475–500 nm (CFP) and 525–540 nm (cpVenus) (Fig. 2a).
2. A non-confocal transmission image is collected in parallel as a bright-field-like reference (Fig. 2a; *see* **Note 9**).

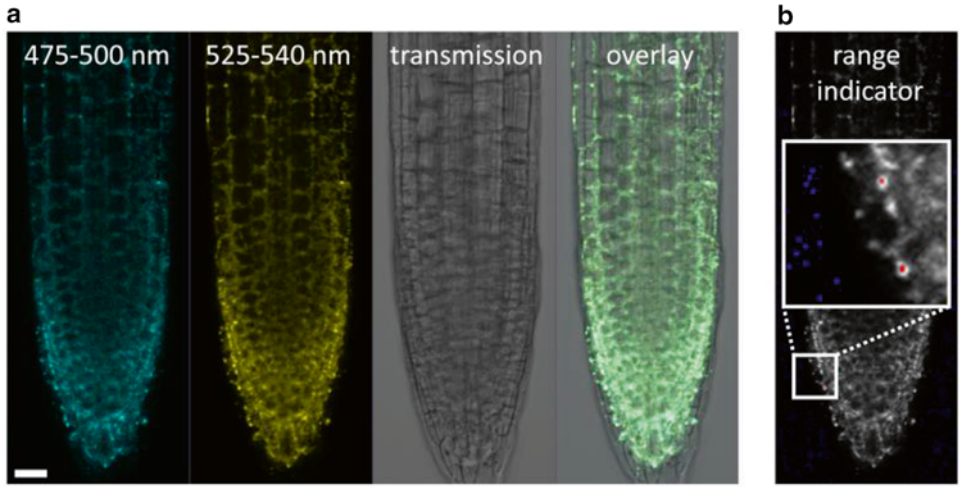

Fig. 2 (**a**) Imaging 4mt-YC3.6 in an Arabidopsis root tip. Channels displayed in *cyan* and *yellow* show emission intensity at 475–500 nm (CFP) and 525–540 nm (cpVenus), respectively, upon excitation at 458 nm using a 25× lens (water immersion, NA 0.8). Size bar = 20 μm. (**b**) Channel showing emission intensity of cpVenus in range indicator mode. Oversaturated and zero pixels are displayed in *red* or *blue*, respectively

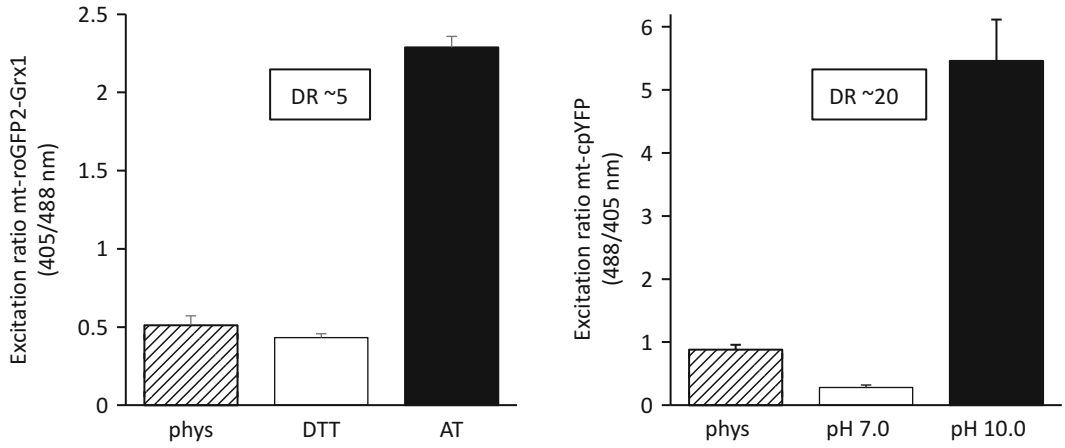

Fig. 3 Exemplary assessment of matrix E_{GSH} and pH in vivo using the mt-roGFP2-Grx1 and mt-cpYFP sensor in root tips of Arabidopsis seedlings. The empirical dynamic spectroscopic range (DR) of the sensors upon in vivo calibration treatments is shown in *insets. phys* physiological state, *DTT* 10 mM dithiothreitol, *AT* 2 mM aldrithiol-2. $n \geq 3$, error bars: SD

3.3 Specific Adjustments for Sensor Imaging

1. Set laser power to ≤30 μW (405 nm) and ≤7 μW (488 nm) for exciting mt-roGFP2-Grx1 and mt-cpYFP, and ≤5 μW (442/458 nm) for 4mt-YC3.6 at the objective. This should be determined empirically with a light meter as there can be large discrepancies between nominal laser power, adjusted output percentage, and the actual power that the sample is exposed

to. Keeping laser exposure low avoids sensor bleaching and minimizes photooxidative stress of the tissue, which can itself affect mitochondrial physiology.

2. Use a detector gain within the linear detector range (≤800). If required the photon yield may be increased at the expense of z-resolution by opening the pinhole up to three Airy units.
3. Select scan speed, pixel resolution, averaging, and digital zoom to generate an image of reasonable visual quality with sufficient signal-to-noise ratio to allow for quantitative measurements.
4. Use simple lookup tables such as the range indicator to adjust the amplifier offset value to completely capture the background signal. This is achieved when only very few zero pixels are apparent in the range indicator mode (Fig. 2b).
5. Avoid pixel saturation as this prevents analysis. This is particularly relevant for mitochondrial localized sensors as the fluorescence signal is highly concentrated in small volumes that can easily reach saturation (Fig. 2b).
6. Choose settings to allow the intensities to change between different images without reaching the detector limits. Anticipate variation in signal intensities due to both differences in sensor expression between individuals, physiologically induced ratio changes, or the full probe response during calibration (*see* **Note 10**).
7. Once optimized, keep the settings strictly constant for a given experiment. Any change of settings will directly impact on the measured ratio.

3.4 Data Collection and Quantitative Image Analysis

1. The simplest type of experiment is to monitor the steady-state effect of a treatment compared to its control condition after a fixed time of exposure. Typically single images are collected for >3 individual root tips per treatment ($n = 10$ recommended). It is helpful if all individuals show comparable sensor expression levels although the ratio approach can compensate for variation in sensor abundance. Images should be recorded at similar tissue depths. Individual root tips that show particularly high autofluorescence signals in the 405 nm channel (for roGFP2-Grx1 and cpYFP) should be avoided.
2. To calibrate the sensor, incubate control seedlings in the respective calibration medium (Table 2), typically for >15 min before image collection, and mount in calibration medium (*see* **Notes 10**–**13**). Collect images for >3 individual root tips per calibration point ($n = 10$ recommended).
3. Load the individual image files into the MatLab-based analysis software and perform the analysis steps in the order set by the program. These include sub-pixel channel alignment, noise reduction and pixel binning, background measurement and

Table 2
Calibration regimes

Sensor	Point 1	Point 2
mt-roGFP2-Grx1	2–5 mM aldrithiol-2, 0.5× MS, 10 mM MES, pH 5.8 (KOH)	10 mM DTT, 0.5× MS, 10 mM MES, pH 5.8 (KOH)
mt-cpYFP	100 mM MOPS-Tris, 40 mM K_2SO_4, 5 µM CCCP, 0.5× MS, pH 7.0	100 mM CHES-Tris, 40 mM K_2SO_4, 5 µM CCCP, 0.5× MS, pH 10.0
4mt-YC3.6 (*see* **Note 11**)	n/a	n/a

subtraction, autofluorescence measurement and subtraction (in case of high autofluorescence in the 405 nm channel), calculation and calibration of the ratio image on a pixel-by-pixel basis, and generation of a pseudo-color representation. Images can be saved in windows .avi format for time series or .tif/.jpg/.png for single images.

4. If required, regions of interest (ROIs) can be manually defined to analyze particular areas and spatial differences. The analysis follows the same sequence as for the generation of the ratio image except that calculations are based on the average intensities in the entire image (or ROI) and provide better signal-to-noise as more pixels are averaged before calculation of the ratio value. The ratio values can be calibrated for conversion to redox potential or pH values (*see* **Note 14**). Export the ratio values as a spreadsheet file (.xls), or a complete output of the graphical data and images as an enhanced metafile (.emf).

4 Notes

1. The sensor must be chosen carefully depending on the hypothesis to be tested. The sensitivity range of the sensor must match the conditions to be assessed. For matrix E_{GSH}, pH, and free calcium levels under control conditions that means that the midpoint potential, pK_a and K_d of the sensor, should be close to −350 mV (note that this value is pH adjusted for matrix pH [13]), 7.8 (our own observation), and 100–200 nM [5, 14], respectively. A number of different variants of the sensors described here are available, but the physiological range they can report is still incomplete.
2. The specificity of the sensor should be well defined, based on in vitro characterization, and ideally be supported by a clear mechanistic understanding of the sensor behavior.

3. The sensor should respond in a ratiometric manner, which allows internal normalization and quantitative measurements independent of sensor expression levels and optical path length variations.
4. The sensor response should be rapid and fully reversible with a known underlying reaction mechanism to ensure a meaningful dynamic readout. For example in the case of roGFPs, fusion to the human glutaredoxin Grx1 increases and standardizes their response kinetics based on a defined reaction mechanism independent of the local intracellular environment of the sensor [15].
5. The sensor should be bright as compared to other components in the plant tissue with similar fluorescence properties, to allow for a high signal-to-noise ratio. This is achieved by a high-fluorescence quantum yield of the sensor as well as reasonable expression levels in the plant cell.
6. The expression of the sensor itself must not affect mitochondrial physiology in any major way. Sufficiently high expression levels are required for a reliable readout with a high signal-to-noise ratio, but each sensor molecule represents an artificial addition to the matrix protein inventory. Matrix homeostasis may be affected by either the high abundance of the additional protein or adding additional buffering capacity for the physiological parameter to be assessed. While there is no consistent empirical indication for the former (many lines overexpressing fluorescent proteins have been produced without any detectable phenotype, e.g. [16]), the latter should be assessed for each specific sensor class and plant line. For instance, the pH active tyrosine of mt-cpYFP contributes to the pH buffering capacity in the physiological range of the matrix. However, one might expect the contribution of mt-cpYFP to matrix pH buffering negligible, given the abundance of endogenous matrix proteins and metabolites. An analogous argument applies for calcium binding by YC3.6 and matrix calcium buffering. Mt-roGFP2-Grx1 expression provides additional protein surface thiols to the matrix, as well as ectopic glutaredoxin activity. For the impact of the sensor on glutathione redox buffering to be minor, the relative abundance of sensor needs to be low as compared to local glutathione concentration, and electron flux through the glutathione pool. This is likely to be the case considering that the estimated sensor expression levels are in the low μM range (our observation), about three orders of magnitude below the estimated matrix glutathione levels (low mM range across the plant cell [17] with indications for even higher levels in the matrix [18]). Nevertheless, interaction of the additional glutaredoxin with endogenous targets cannot be ruled out.

7. Correct localization of the sensor in the mitochondria must be unambiguous. Mis-localization in the cytosol or in the plastids is not uncommon for strongly expressed fluorescent proteins and must be either ruled out by selection of appropriate lines or considered appropriately in the experiment [7].
8. Silencing of sensor expression giving rise to tissue with patchy expression or absent fluorescence can be problematic and often increases over generations. Preselection of individuals to be used for experiments by fluorescence, rather than antibiotic resistance, is advisable. Depending on the question, tissues with patchy sensor expression may be still usable for data collection as long as parts of the image contain clear signal.
9. If images are collected in green tissues a channel should be added to monitor chlorophyll fluorescence (excitation 405, 442, 458, or 488 nm; emission 640–700 nm) and to make sure that chlorophyll signal does not bleed through into any of the channels used for ratioing. This is particularly relevant if stress treatments are applied which may affect the chloroplast fluorescence spectrum.
10. In vivo sensor calibration by a standardized regime is an important, yet not always straightforward, element of a meaningful experiment. It (a) ensures that the sensor construct responds in a manner that is comparable to its in vitro behavior, (b) sets the maximal spectroscopic dynamic range within which the sensor can respond under the present conditions, and (c) allows calculation of absolute concentrations from the ratio data (*see* **Note 14**). The minimal requirement for an in vivo calibration is to drive the sensor to its two extremes with high confidence (i.e., fully protonated/deprotonated, oxidized/reduced, occupied/free binding site). Ideally, a full titration through the midpoint would be valuable, but can be difficult to achieve for routine measurements. Here we describe calibration regimes for mitochondrial pH and E_{GSH}.
11. In vivo calibration of 4mt-YC3.6 has been attempted using 5 mM EGTA and 10 mM $CaCl_2$, respectively, in the presence of the calcium ionophores ionomycin or A23187, but the sensor could not be driven to the expected extreme ratios (our own observations). Since the sensor responds to calcium stimuli nevertheless, it is likely that the ionophores do not reach the relevant membranes *in planta*. Currently no reliable calibration regime for mitochondrial YC3.6 is available for intact plant tissues.
12. Full oxidation of roGFP2 sensors can be achieved with 10–100 mM H_2O_2 [13, 19]. While that regime drives the sensor into oxidation, it can lead to partial sensor bleaching, formation of oxygen bubbles that interfere with imaging, and cell

death. In addition its efficient detoxification by the antioxidant defense machinery of the plant cell can leave doubts if the sensor has really been fully oxidized. This can be avoided by specific thiol oxidation with aldrithiol-2 (2,2′-dipyridyl disulfide) [20, 21] as suggested here.

13. In young seedlings tissue penetration by the calibration agents suggested here has been found unproblematic. This is likely to differ for other tissues and requires optimization.
14. Based on the calibration and the midpoint redox potential, pK_a and K_d (and Hill coefficient) of the sensor, respectively, an absolute value of redox potential, pH, or calcium concentration can be calculated. This value will not only depend on accurate calibration values, but also on additional parameters. For instance, the redox potential depends on the local pH environment, which needs measurement or estimation. In addition an assumption has to be made that the midpoint potential of the sensor does not differ between in vitro and in vivo conditions. While this is a reasonable assumption for a lot of fluorescent protein sensors, unexpected behavior in a complex in vivo situation can not be fully ruled out. Nevertheless a relative comparison between samples is possible without further transformation of the ratio values and avoids potential calibration-related artifacts.

Acknowledgement

M.S. was supported by the Deutsche Forschungsgemeinschaft through the Emmy Noether Programme (SCHW1719/1-1).

References

1. Baradaran R, Berrisford JM, Minhas GS et al (2013) Crystal structure of the entire respiratory complex I. Nature 494:443–448
2. Schwarzländer M, Finkemeier I (2013) Mitochondrial energy and redox signaling in plants. Antioxid Redox Signal 18:2122–2144
3. Schwarzländer M, Fricker MD, Sweetlove LJ (2009) Monitoring the in vivo redox state of plant mitochondria: effect of respiratory inhibitors, abiotic stress and assessment of recovery from oxidative challenge. Biochim Biophys Acta 1787:468–475
4. Poburko D, Santo-Domingo J, Demaurex N (2011) Dynamic regulation of the mitochondrial proton gradient during cytosolic calcium elevations. J Biol Chem 286:11672–11684
5. Loro G, Drago I, Pozzan T et al (2012) Targeting of Cameleons to various subcellular compartments reveals a strict cytoplasmic/mitochondrial Ca^{2+} handling relationship in plant cells. Plant J 71:1–13
6. Imamura H, Nhat KP, Togawa H et al (2009) Visualization of ATP levels inside single living cells with fluorescence resonance energy transfer-based genetically encoded indicators. Proc Natl Acad Sci U S A 106:15651–15656
7. Albrecht SC, Sobotta MC, Bausewein D et al (2014) Redesign of genetically encoded biosensors for monitoring mitochondrial redox status in a broad range of model eukaryotes. J Biomol Screen 19:379–386
8. Schwarzländer M, Logan DC, Fricker MD et al (2011) The circularly permuted yellow fluorescent protein cpYFP that has been used as a superoxide probe is highly responsive to pH but not superoxide in mitochondria: implications

for the existence of superoxide 'flashes'. Biochem J 437:381–387

9. Behera S, Krebs M, Loro G et al (2013) Ca^{2+} imaging in plants using genetically encoded Yellow Cameleon Ca^{2+} indicators. Cold Spring Harb Protoc 2013:700–703
10. Schwarzländer M, Logan DC, Johnston IG et al (2012) Pulsing of membrane potential in individual mitochondria: a stress-induced mechanism to regulate respiratory bioenergetics in Arabidopsis. Plant Cell 24:1188–1201
11. Loro G, Costa A (2013) Imaging of mitochondrial and nuclear Ca^{2+} dynamics in Arabidopsis roots. Cold Spring Harb Protoc 2013:781–785
12. Costa A, Candeo A, Fieramonti L et al (2013) Calcium dynamics in root cells of *Arabidopsis thaliana* visualized with selective plane illumination microscopy. PLoS One 8:e75646
13. Schwarzländer M, Fricker MD, Müller C et al (2008) Confocal imaging of glutathione redox potential in living plant cells. J Microsc 231: 299–316
14. Logan DC, Knight MR (2003) Mitochondrial and cytosolic calcium dynamics are differentially regulated in plants. Plant Physiol 133:21–24
15. Gutscher M, Pauleau AL, Marty L et al (2008) Real-time imaging of the intracellular glutathione redox potential. Nat Methods 5:553–559
16. Logan DC, Leaver CJ (2000) Mitochondria-targeted GFP highlights the heterogeneity of mitochondrial shape, size and movement within living plant cells. J Exp Bot 51: 865–871
17. Fricker MD, May M, Meyer AJ et al (2000) Measurement of glutathione levels in intact roots of Arabidopsis. J Microsc 198:162–173
18. Zechmann B, Mauch F, Sticher L et al (2008) Subcellular immunocytochemical analysis detects the highest concentrations of glutathione in mitochondria and not in plastids. J Exp Bot 59:4017–4027
19. Marty L, Siala W, Schwarzländer M et al (2009) The NADPH-dependent thioredoxin system constitutes a functional backup for cytosolic glutathione reductase in Arabidopsis. Proc Natl Acad Sci U S A 106:9109–9114
20. Dooley CT, Dore TM, Hanson GT et al (2004) Imaging dynamic redox changes in mammalian cells with green fluorescent protein indicators. J Biol Chem 279:22284–22293
21. Ostergaard H, Tachibana C, Winther JR (2004) Monitoring disulfide bond formation in the eukaryotic cytosol. J Cell Biol 166: 337–345
22. Meyer AJ, Brach T, Marty L et al (2007) Redox-sensitive GFP in *Arabidopsis thaliana* is a quantitative biosensor for the redox potential of the cellular glutathione redox buffer. Plant J 52:973–986
23. Nagai T, Sawano A, Park ES et al (2001) Circularly permuted green fluorescent proteins engineered to sense Ca^{2+}. Proc Natl Acad Sci U S A 98:3197–3202
24. Wang W, Fang H, Groom L et al (2008) Superoxide flashes in single mitochondria. Cell 134:279–290
25. Nagai T, Yamada S, Tominaga T et al (2004) Expanded dynamic range of fluorescent indicators for Ca^{2+} by circularly permuted yellow fluorescent proteins. Proc Natl Acad Sci U S A 101:10554–10559
26. Filippin L, Abad MC, Gastaldello S et al (2005) Improved strategies for the delivery of GFP-based Ca^{2+} sensors into the mitochondrial matrix. Cell Calcium 37:129–136
27. Schwarzländer M, Wagner S, Ermakova YG et al (2014) The 'mitoflash' probe cpYFP does not respond to superoxide. Nature 514(7523):E12–E14. doi:10.1038/nature13858